Sensors and Materials, Vol. 10, No. 3 (1998) 129–138
MYU Tokyo

S & M 0319

Pressure Sensor Using Shear Piezoresistance of Polysilicon Films

Sung-June Park and Se-Kwang Park[1]

Technical Center, Daesung Electric Co., LTD.,
743-5, Wonsi-Dong, Ansan-City, Kyunggi-Do (B/L 8-27), Korea
[1] Department of Electrical Engineering, Kyungpook National University,
1370 Buk-Ku, Sankyuk-Dong, Taegu 702-701, Korea

(Received September 11, 1996; accepted January 5, 1998)

Key words: pressure sensor, polysilicon films, shear piezoresistive effect

This paper presents the characteristics of a pressure sensor incorporating a shear-type piezoresistor of low-pressure chemical vapor deposition (LPCVD)-grown polysilicon films. The sensor has 3.1 mV/V of pressure sensitivity in the pressure range of 1 kgf/cm^2, and ± 0.03%FS/°C of temperature coefficient of offset (TCO), and ± 0.15%FS/°C of temperature coefficient of sensitivity (TCS) in the temperature range of –20 ~ +125°C. It showed ± 0.2%FS of hysteresis and ± 1.5%FS of non-linearity. The shear-type polycrystalline silicon pressure sensor can eliminate the temperature dependence of offset caused by a mismatch of resistors and can be used in a relatively wide temperature range, compared to conventional full-bridge silicon pressure sensors.

1. Introduction

The conventional pressure sensor has been widely used in the form of a Wheatstone bridge using the piezoresistive effect of single crystalline silicon. The researches on four-terminal pressure sensor using the shear piezoresistive effect, which have fabrication and design advantages including diaphragm minimization, have also been carried out.[1,2] The shear piezoresistive effect is development of voltage drop which is proportional to stress in the case where the electric field is perpendicular to the current direction and the function of angle between resistor and stress direction in a cubic crystal. This effect has the same function as that of Hall effect in magnetic field and was introduced by Pfann and Thurston in their study of the longitudinal and transverse piezoresistive effect of single crystalline

silicon.[1]

A single element four-terminal pressure sensor has the advantages of a high gauge factor and alleviation of the TCO caused by mismatch of resistors which exists in the Wheatstone bridge-type sensor. Since the temperature dependence of the offset voltage and piezoresistive coefficients still exists, limitation of operating temperature and temperature compensation are needed.

To solve these problems, we fabricated and tested the pressure sensor using thermally diffused polysilicon piezoresistor. The shear piezoresistive effect of polysilicon films was theoretically analyzed in this study.

2. Shear Piezoresistance of Polysilicon Films

In a single element four-terminal resistor with a current density j_x in the direction x as shown in Fig. 1, the electric field E_y developed in the direction y is written as the function of corresponding piezoresistive coefficients and stresses in each direction as

$$\frac{\Delta E_y}{\rho_o j_x} = \pi'_{61}\sigma'_x + \pi'_{62}\sigma'_y + \pi'_{66}\tau'_{xy}, \tag{1}$$

where ρ_o is the resistivity of the resistor, σ'_x and σ'_y are the normal stresses, and τ'_{xy} is the shear stress. π'_{61}, π'_{62} and π'_{66} are perpendicular electric fields developed for each stress and can be written as

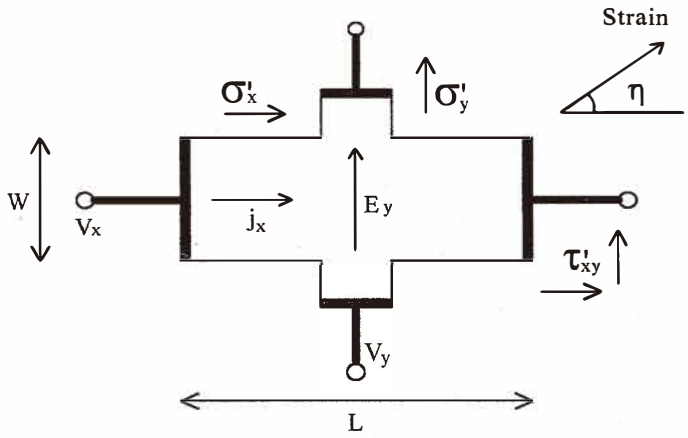

Fig. 1. Four-terminal resistor and stresses in each direction.

$$\pi'_{61} = 2(\pi_{11} - \pi_{12} - \pi_{44})(l_1^3 l_2 + m_1^3 m_2 + n_1^3 n_2)$$

$$\pi'_{62} = 2(\pi_{11} - \pi_{12} - \pi_{44})(l_1 l_2^3 + m_1 m_2^3 + n_1 n_2^3)$$

$$\pi'_{66} = \pi_{44} + 2(\pi_{11} - \pi_{12} - \pi_{44})(l_1^2 l_2^2 + m_1^2 m_2^2 + n_1^2 n_2^2),$$

where l_i, m_i and n_i are the directional cosines in the axis rotation, and π_{11}, π_{12} and π_{44} are piezoresistive coefficients of the unstressed resistor.

The structure of polysilicon film can be simplified by modification of the grain and grain boundary which is the transition region of adjacent grains as shown in Fig. 2, and the total resistivity ρ can be given by[3]

$$\rho = \frac{\ell - (2w + \delta)}{\ell}\rho_g + \frac{2w + \delta}{\ell}\rho_b, \tag{2}$$

where ρ_g is a grain resistivity, ρ_b is a grain boundary resistivity, ℓ is a grain size, w is a grain boundary size and δ is a depletion region size.

Considering the grain and grain boundary separately, the change of resistivity $\Delta\rho/\rho$ can be written as

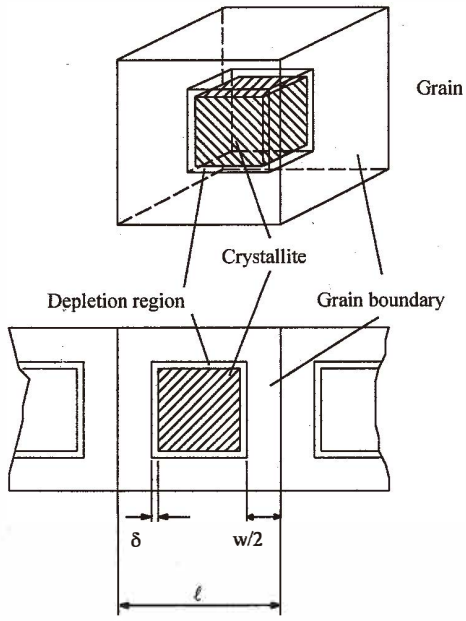

Fig. 2. Model of polysilicon crystals.

$$\frac{\Delta\rho}{\rho\varepsilon} = \frac{\ell-(2w+\delta)}{\ell\varepsilon\rho}\Delta\rho_g + \frac{2w+\delta}{\ell\varepsilon\rho}\Delta\rho_b, \tag{3}$$

where $\Delta\rho_g$ and $\Delta\rho_b$ are the changes in grain and grain boundary respectively, and ε the strain. Because the term on the left-hand side of eq. (3) represents the gauge factor, it can be rewritten, using S'_{ii} which is a compliance coefficient for strain parallel to stress as[4]

$$\frac{\pi}{S'_{ii}} = \frac{\Delta\rho}{\rho\varepsilon} = \frac{1}{S'_{ii}}\left[\frac{\rho_g\pi_{1g}}{\rho_g + \dfrac{2w+\delta}{\ell-(2w+\delta)}\rho_b} + \frac{\rho_b\pi_{1b}}{\dfrac{\ell-(2w+\delta)}{2w+\delta}\rho_g + \rho_b}\right], \tag{4}$$

where $S'_{ii} = S_{11} + (S_{44} + 2S_{12} - 2S_{44})(l_i^2 m_i^2 + l_i^2 n_i^2 + m_i^2 n_i^2)$, and π_l, π_{lg} and π_{lb} are the longitudinal piezoresistive coefficients of polysilicon film, grain and grain boundary, respectively.

Equation (4) derives a piezoresistive coefficient of each grain, and taking into account this equation the gauge factor of grain can be expressed as

$$G = 1 - \sum_j \frac{S'_{ij}}{S'_{ii}}(1-\delta_{ij}) + \frac{1}{S'_{ii}}\left[\frac{\rho_g\pi_{1g}}{\rho_g + \dfrac{2w+\delta}{\ell-(2w+\delta)}\rho_b} + \frac{\rho_b\pi_{1b}}{\dfrac{\ell-(2w+\delta)}{2w+\delta}\rho_g + \rho_b}\right], \tag{5}$$

where $S'_{ij} = S_{12} + (S_{11} - S_{12} - 1/2S_{44})(l_i^2 l_j^2 + m_i^2 m_j^2 + n_i^2 n_j^2)$.

To determine the gauge factor of polysilicon resistor, the orientation of each grain must be considered because polysilicon consists of grains which have different orientations. Actually, the gauge factor depends on not only the impurity concentrations but also dominated orientations which have complicated structures.[5]

The output voltage ΔV_y of the four-terminal polysilicon resistor corresponding to the applied voltage V_x and stress ε is given by[6]

$$\frac{\Delta V_y}{V_x\varepsilon} = \frac{W}{L}\frac{\rho_g}{\rho}\left(\frac{\pi'_g}{S'_{ii}} + \frac{2w+\delta}{\ell-(2w+\delta)}\frac{\pi'_{ba}}{S'_{ii}}\right), \tag{6}$$

where L and W are dimensions of the four-terminal resistor shown in Fig. 1, π'_g and π'_{ba} are the transverse voltage piezoresistive coefficients for the grain and along the barrier, respectively.

3. Design and Fabrication

The fabricated sensor was designed to be as a rectangular type in which the anisotropic property of the polysilicon gauge factor and the wet etching process were considered as shown in Fig. 3. Using the finite element method, the stress of the aspect ratio (*b*/*a*) of the silicon diaphragm was calculated. In Fig. 4, the normalized stress at the center and edge of the diaphragm has a maximum value when the aspect ratio is 2.[7] Therefore, the diaphragm size of the sensor was designed to be 1500 μm × 3000 μm. Pressure sensitivity is affected by the stress distribution of the diaphragm on which piezoresistors are located. The stress distributions along the x and y-axes are given as[8]

$$\sigma_x = \frac{-Eh}{2(1-\nu^2)}\left(\frac{\partial^2 D}{\partial x^2} + \nu\frac{\partial^2 D}{\partial y^2}\right)$$
$$\sigma_y = \frac{-Eh}{2(1-\nu^2)}\left(\frac{\partial^2 D}{\partial y^2} + \nu\frac{\partial^2 D}{\partial x^2}\right), \tag{7}$$

where E is the Young's modulus of silicon, ν is the Poisson's ratio and D is a deflection of the diaphragm. Figure 5 shows curves of the calculated stress distribution of the rectangular diaphragm.

Since $|\sigma_x - \sigma_y|$ has a maximum value at the edge and center along the width and length

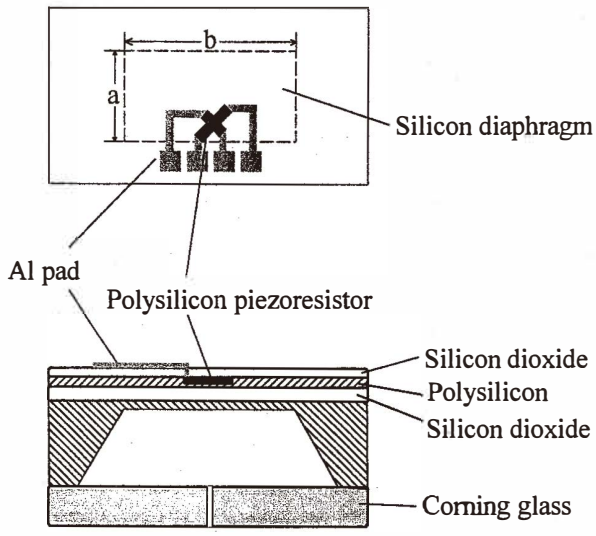

Fig. 3. Cross section and top view of pressure sensor.

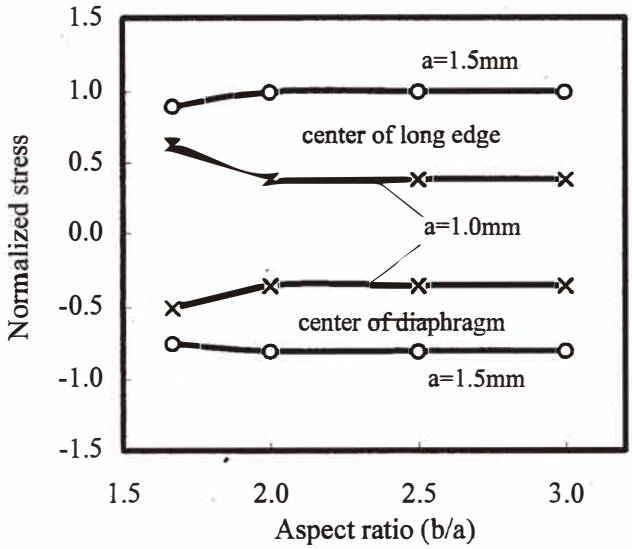

Fig. 4. Normalized stress on the diaphragm according to aspect ratio of rectangular diaphragm.

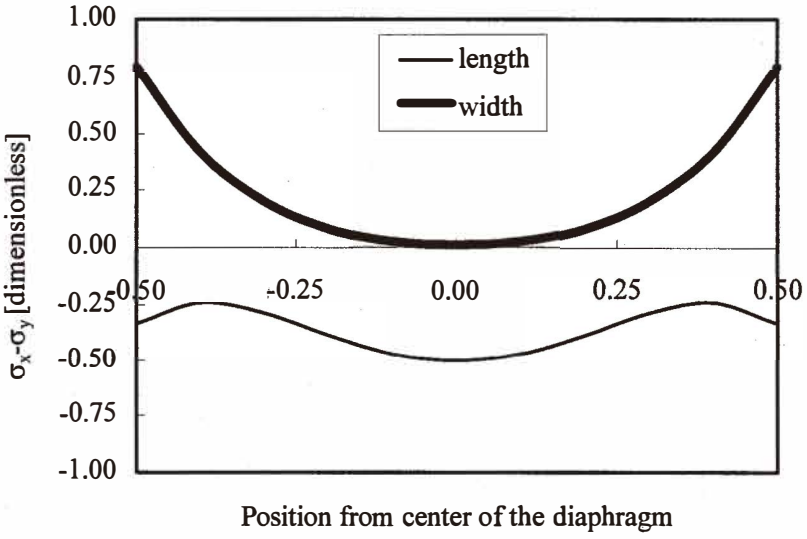

Fig. 5. Values of ($\sigma_x - \sigma_y$) along the length and width of diaphragm.

of the diaphragm respectively, the piezoresistor was positioned at the middle edge of the diaphragm.

The fabrication process of the pressure sensor includes integrated-circuit and micromachining technologies such as chemical etching and anodic bonding. The base material is n-type 300-μm-thick silicon substrate with 1.2-μm-thick silicon dioxide layer fabricated on it by thermal oxidation. Subsequently, polysilicon films of 5000 Å thickness are deposited onto silicon wafers by LPCVD at 625°C. During the deposition process, using SiH_4 as reaction gas, the chamber pressure was 0.5 Torr and the growth rate was about 80 Å/min. For patterning of the films, silicon dioxide was grown again by wet thermal oxidation. After formation of p-type piezoresistors by thermal diffusion of Boron at 1000°C, contact holes were patterned through the silicon dioxide layer. The patterning was completed by connecting the resistor using evaporated aluminum. The impurity concentration of diffused polysilicon was about $2.0 \times 10^{19}/cm^3$.

Using tetra methyl ammonium hydroxide (TMAH) 22 wt% solution at 90°C, the silicon diaphragm was chemically etched in the jig to control the thickness. To detect the unetched diaphragm thickness, the principle of light penetration through silicon diaphragm below thickness of 30 μm was used. The sensors were anodically bonded at a temperature of 400°C and voltage of 950 V DC using Corning #7740 glass for the reference cavity. The dimensions of the whole sensor are 4 mm × 5 mm × 300 μm. Finally, the sensor was packaged in a metal can and Al wire was used to connect the sensor pad and pin of the can. Figure 6 shows a photograph of the patterned sensor.

4. Results and Discussion

Nitrogen gas was used as pressure source to measure characteristics of the fabricated sensor. A reference pressure gauge model PPC2 of DH INSTRUMENT, having 0.05% accuracy, was employed. To accurately maintain the temperature at a fixed level, the oven of model S-1.2C (THERMOTRON) was employed, which has a temperature range of $-73 \sim +177$°C and a tolerance of temperature variation of ± 0.3°C. Exciting voltage of 5 V DC was supplied to the sensor by HEWLETT PACKARD 6543A. Output voltage of the sensor was measured at pressure points of 0.0, 0.2, 0.4, 0.6, 0.8 and 1.0 kgf/cm^2, and temperature points of -20, $+25$, $+80$ and $+125$°C.

Figure 7 shows the change in output voltage in the pressure range of 0.0 ~ 1.0 kgf/cm^2 at room temperature. In the curve, the sensor showed 3.1 mV/V of pressure sensitivity and ± 1.5%FS/°C of nonlinearity. Figures 8 and 9 represent the changes in hysteresis and nonlinearity according to the temperature range, respectively. As the temperature rises and falls, the hysteresis of the sensor increases, and the nonlinearity decreases. The temperature coefficient of offset is $\pm$ 0.03%FS/°C, and temperature coefficient of sensitivity is $\pm$ 0.15%FS/°C, as shown in Fig. 10. These values represent much better temperature properties than those of the pressure sensor made of single crystalline silicon.

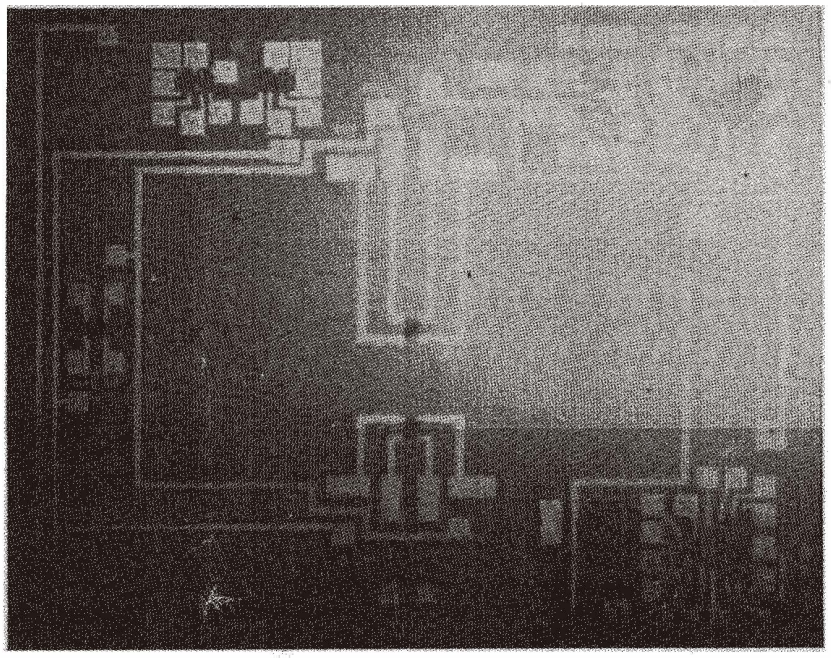

Fig. 6. Photograph of fabricated sensor pattern.

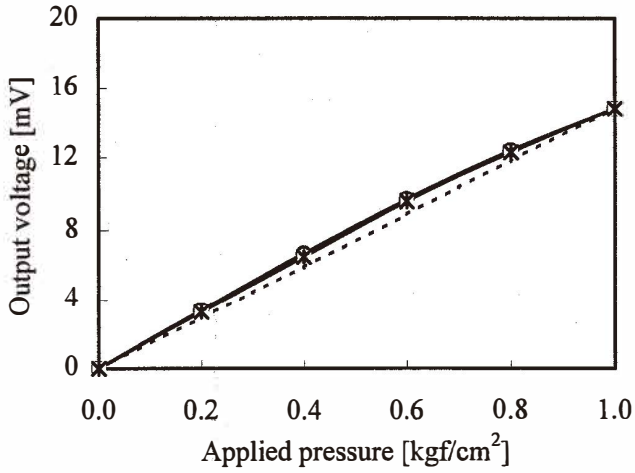

Fig. 7. Characteristics of pressure sensitivity.

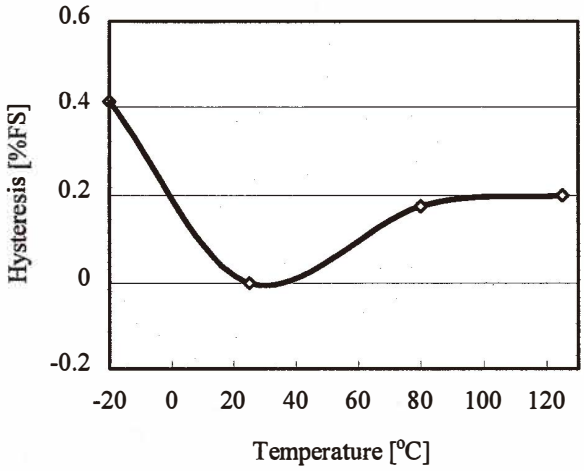

Fig. 8. Hysteresis of sensor output according to temperature.

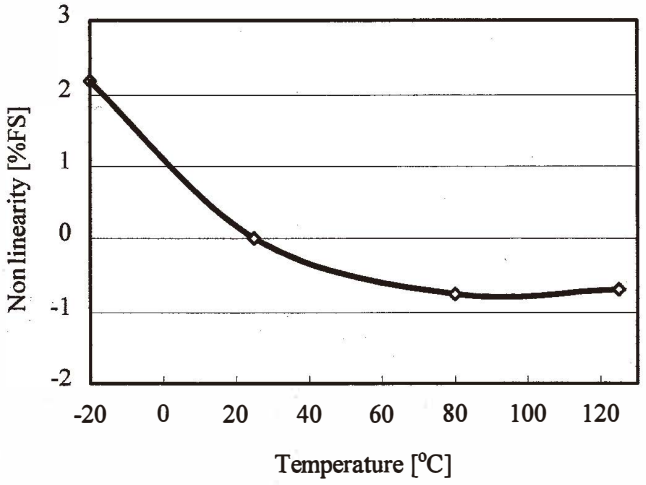

Fig. 9. Nonlinearity of sensor output according to temperature.

5. Conclusions

In this paper, the properties of a pressure sensor which combined the temperature characteristics of polysilicon and a four-terminal piezoresistor were evaluated. Although the fabricated sensor has 30% of the pressure sensitivity of a Wheatstone bridge-type

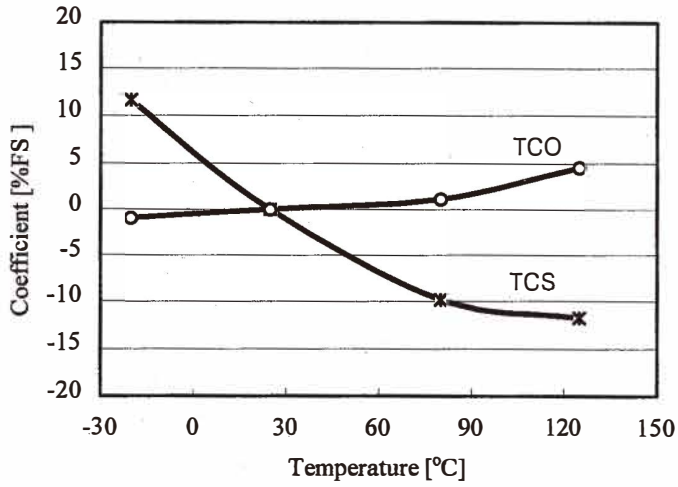

Fig. 10. TCS and TCO characteristics of the pressure sensor.

sensor, it can alleviate the errors caused by mismatch of resistor and can be used stably in a wider temperature range.

In the range of – 20 ~ +125°C, the results showed very low temperature dependence of TCO (± 0.03%FS/°C) and TCS (± 0.15%FS/°C). These values represent the capability of operation without temperature compensation. Since the polysilicon four-terminal pressure sensor evaluated in this paper has a good temperature property with a basic ability for measuring pressure, it can solve the limitations of a pressure sensor used under high-temperature operations such as in industrial and automotive applications.

Further studies related to gauge factor of polysilicon and orientation dependency are required for a better understanding of the properties of the sensor.

References

1 W. G. Pfann and R. N. Thurston: J. Appl. Phys. **32** (1961) 2008.
2 Y. Kanda and A. Yasukawa: Sensors and Actuators **2** (1982) 283.
3 N. C. C. Lu, L. Gertzberg, C. Y. Lu and J. D. Meindl: IEEE Trans. Electron Devices **ED-28** (1985) 818.
4 P. J. French and A. G. R. Evans: Sensors and Actuators **8** (1985) 219.
5 T. I. Kamins: J. Electrochem. Soc.: SOLID- STATE SCIENCE AND TECHNOLOGY **127** (1980) 686.
6 P. J. French and A. G. R. Evans: Sensors and Actuators **15** (1988) 257.
7 Y. T. Lee, H. D. Seo, R. Takano, Y. Matsumoto, M. Ishida and T. Nakamura: Sensors and Materials **7** (1995) 53.
8 X. P. Wu, M. F. Hu, J. Y. Shen and Qi. H. Ma: Sensors and Actuators A**35** (1993) 197.